The International Journal of Biochemistry & Cell Biology 65 (2015) 12–19

Contents lists available at ScienceDirect

The International Journal of Biochemistry & Cell Biology

journal homepage: www.elsevier.com/locate/biocel

5 regulates zebrafish yolk extension by suppressing a p53-dependent DNA damage response pathway

Yixing Zhai[a,c,d], Xinyuan Zhao[a,c,d], Jinghao Sheng[a,c,d], Xiangwei Gao[a,c,d], Zhao Ou[e], Zhengping Xu[a,b,c,d,*]

[a] I E H , H , H 310058, C
[b] C I C D I D , , H 310003, C
[c] M C B , M , H 310058, C
[d] C M M , M , H 310058, C
[e] K L M A , M E , C A ,

induces yolk extension defects and massive apoptosis especially in the primary head region (Chakraborty et al., 2009). Here, we report a new yolk extension regulator 5 and its mechanism of action underlying its activity.

2. Materials and methods

2.1. F

Zebrafish fish lines (wild type AB line and 53[M214K]) were maintained in the fish facility at the Key Laboratory for Molecular Animal Nutrition, Ministry of Education, Zhejiang University College of Animal Sciences and in compliance with Institute Animal Care and Use Committee (IACUC).

2.2. A C (C)

Total RNA was extracted from embryos using TRIzol reagent (Invitrogen). Then reverse transcription was performed by Superscript II reverse transcription kit (Invitrogen). Then, the quantitative real-time PCR were performed with specific primers listed in Table 1. The PCR products were confirmed by DNA sequencing.

2.3. A in situ (I H)

To visualize the expression pattern of 5, we used digoxigenin (DIG)-labeled full-length 5 mRNA as probe to carry out WISH analysis. Embryos were fixed in 4% paraformaldehyde (PFA), hybridized with the DIG-labeled RNA probe in hybridization buffer at 68 °C, and then incubated with anti-DIG antibody conjugated with alkaline phosphatase (AP). After staining with Nitroblue Tetrazolium/5-Bromo-4-chloro-3-Indolyl Phosphate (NBT/BCIP) substrate solution, the embryos were observed with VH-M100 Microscopy System. To do WISH on cryosections, we first fixed the embryos in 4% PFA and cryosectioned them after embedded with low-melting agarose gel and optimum cutting temperature compound. The slides were hybridized as described above.

2.4. M (M) A

Two 5 antisense MOs were designed and used in the present study: MO-1: 5′-CGGCAGACTGAAGAATCTCCATGAC-3′, which specifically targets ATG region of 5; MO-2: 5′-TTGTAAGTGAACCCCAACCTTGCTT-3′, which targets the 5′UTR of 5. The sequence of the standard control MO is 5′-CCTCTTACCTCAGTTACAATTTATA-3′. p53 MO sequence (5′-GCGCCATTGCTTTGCAAGAATTG-3′) was adopted as previously described that targets the p53 ATG region (

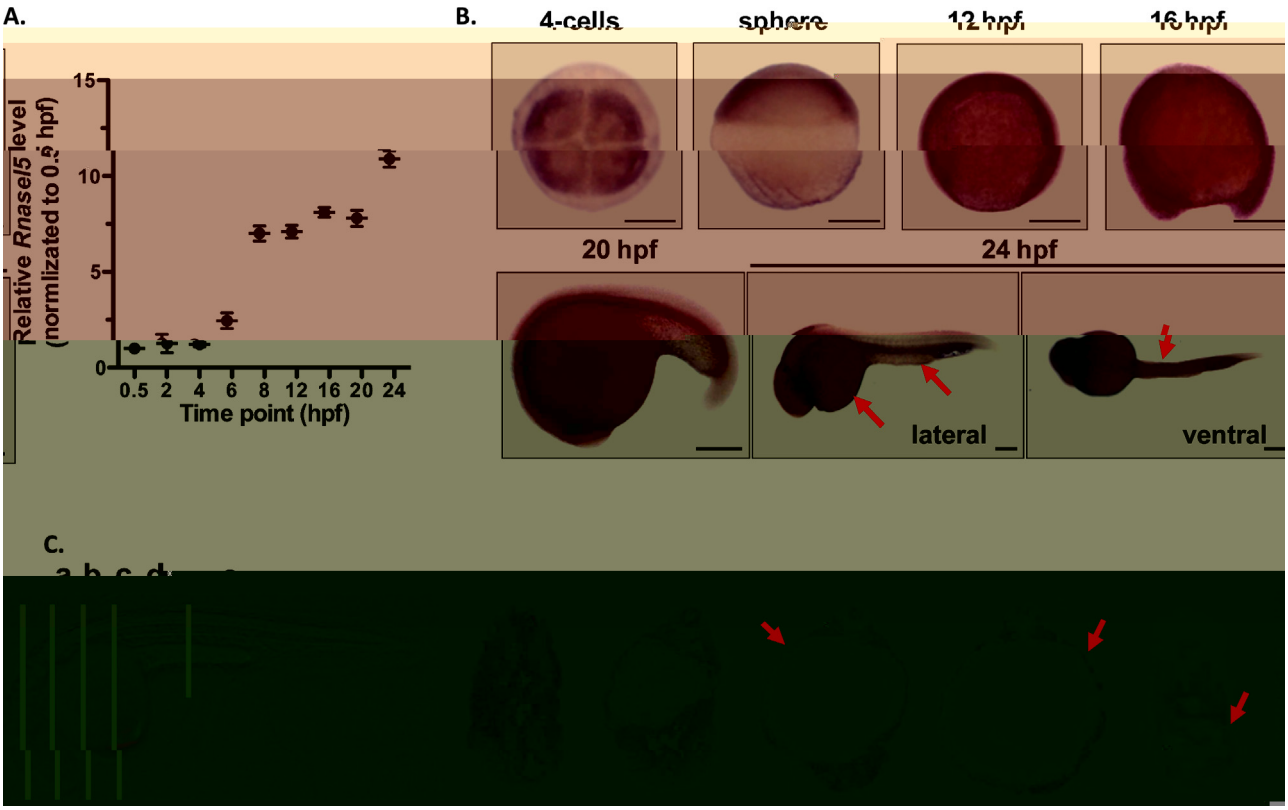

Fig. 1. Temporal and spatial expression patterns of *5* during early embryonic development in zebrafish. (A) RT-qPCR assay was performed to detect *5* expression level from 0.5 hpf to 24 hpf. (B) Spatial expression patterns of *5* at different stages were detected by WISH. The red arrows show *5* located on the anterior–posterior embryonic axis and the ventral of the trunk at 24 hpf, scale bar 100 μm. (C) Cross sections of WISH in left panel embryo as indicated by yellow line. Red arrow indicates *5* located in the overlying layers of yolk, scale bar 100 μm. (For interpretation of the references to color in this figure legend, the reader is referred to the web version of the article.)

Monitoring the embryos treated with different morpholinos at early time points revealed a defect in hatching in *5* morphants. For example, at 2.5 dpf, 97% of embryos treated with control MO hatched, while only 1.7% of MO-1-treated and 4.3% of MO-2-treated ones hatched (Fig. 2D). The failure of hatching or delay to hatch resulted in a decreased survival at a later time point. Compared to the control MO injected embryos that showed a >80% (42/53) survival at 5 dpf, only <34% (22/64) of MO-1 and <50% (27/54) MO-2 embryos survived (Fig. 2E). More severely, the *5* MOs-injected embryos could hardly survive to the time point of 7 dpf, suggesting that *5* knockdown is embryonic lethal. Significantly, the defects in development caused by *5* knockdown can be, at least partially, rescued by a co-injection of the *5* mRNA (Fig. 2D and E). As the human homolog of *5* is related to angiogenesis (Gao and Xu, 2008; Pizzo et al., 2011; Sheng et al., 2014), we continued to examine the effect of *5* on angiogenesis in transgenic zebrafish line Tg (*fl 1*:EGFP)^{y1}, which expresses enhanced GFP in the entire vasculature under the control of the fli1 promoter. Our results showed that most of the intersegmental vessels (ISVs) failed to sprout from the dorsal aorta (DA) at 24 hpf in *5* morphants, while ISVs had sprouted already and extended above the horizontal myoseptum at the same time point in control embryos, indicating *5* plays an important role in zebrafish angiogenesis (Fig. 2F).

3.3. *K* Rnasel5

Interestingly, we found that the major defects in *5* morphants were in the yolk extension region. Yolk extension development starts from 14-somite stage at 16 hpf and extends to primary larvae at 24 hpf. The yolk extension showed slightly difference between control group and *5* morphants at the middle stage of somitegenesis (20 hpf) (Fig. 3A, left panel). However, severe yolk extension defects, even complete disappearance of yolk extension, were observed in *5* morphants at 24 hpf (Fig. 3A, right panel). To confirm our observation, hematoxylin and eosin staining (H&E staining) on cryosections of the 24 hpf embryos were performed. As shown in Fig. 3B, the cross-sectional area of yolk extension was reduced in *5* morphants. The yolk extension defects can be partially rescued by co-injecting *5* mRNA. Quantitative analyses of these phenotypes were also carried out and shown in Fig. 3C and D. These results indicated that the maintenance of yolk extension was severely affected by the depletion of *5*.

3.4. Rnasel5
D A L

The formation and maintenance of yolk extension correlates with the yolk syncytial layer and external tissue layers including the mesendodermal mantle, the embryonic epidermis, and the EVL (Lyman Gingerich et al., 2006). It is possible that the changes in the overlying layers of yolk are associated with yolk extension defect. In addition, angiogenin/Rnase5 (RNASE5), the human homologous gene of *5*, has been shown to regulate cellular apoptosis (Li et al., 2010; Sadagopan et al., 2012). Therefore, we carried out TUNEL assay on the cryosections of *5* morphants, mRNA rescue group and control group at 24 hpf. Almost no TUNEL positive nuclei was detected in the control group; however, significant amount of TUNEL-positive nuclei was observed in the overlying layers of the yolk from *5* morphants, while decreased again in mRNA-rescue group (Fig. 4A–D). To reveal which layer did the

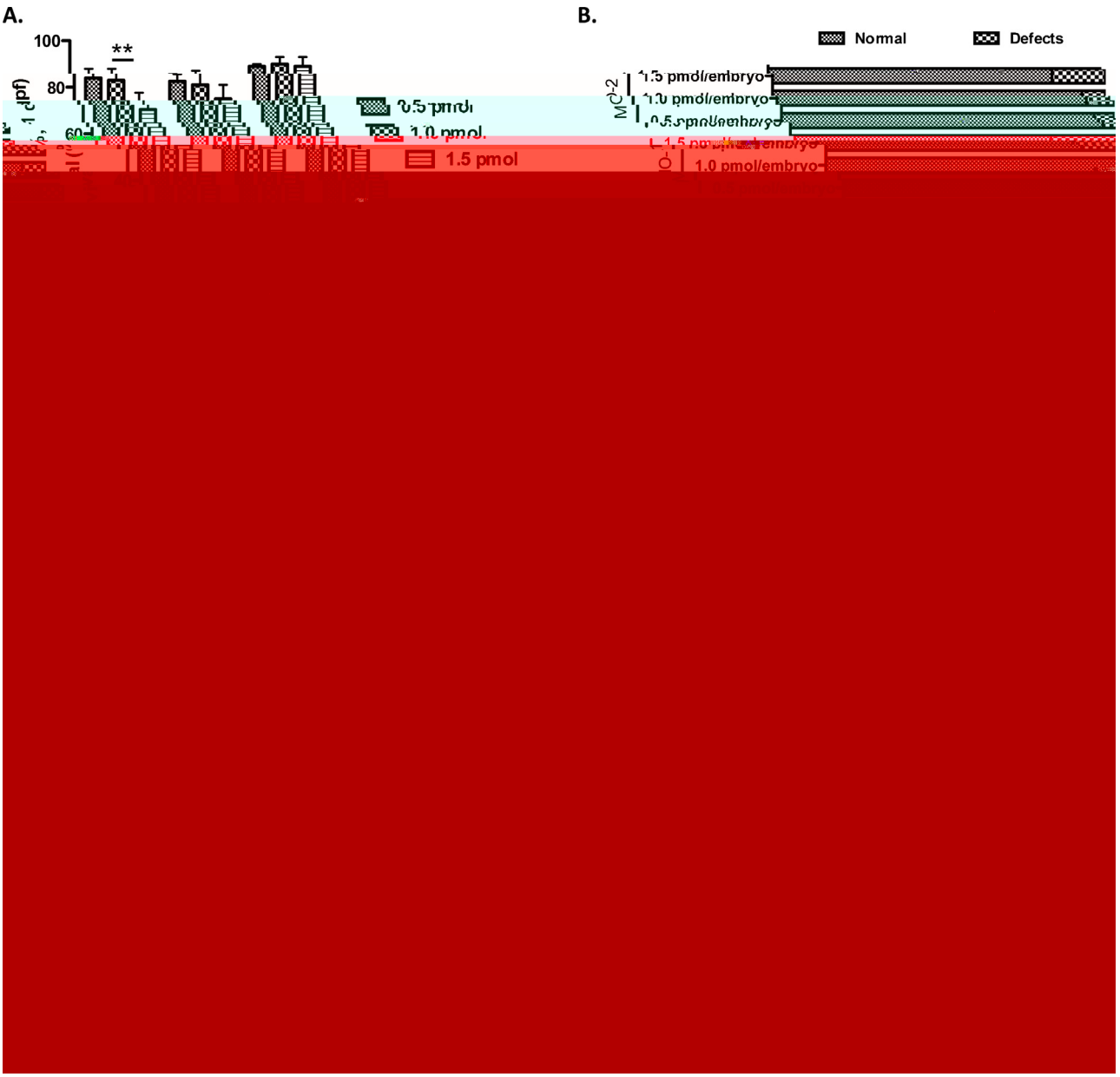

Fig. 2. The effects of *5* depletion on zebrafish. (A and B) Optimization of *5* MO's concentration. The survival rates (A) and teratogenesis (B) of embryos were analyzed after treating with different concentration of MOs at 1 dpf. (C) The efficiencies of *5* MOs. The GFP expression level of EGFP-tag reporter was decreased after co-injecting with MOs, scale bar 100 μm. (D) Hatching time and rates of embryos under different treatment. (E) The survival rates of embryos treated with MOs at 5 dpf. (F) The effect of *5* on sprouting of intersegmental vessels (ISVs) in Tg (*fl 1*:EGFP)^{y1}. Embryos injected *5* MO-1 and control MO were observed under fluorescence microscope. The red arrow shows the ISVs of zebrafish. The red dotted line shows the horizontal myoseptum of zebrafish, scale bar 100 μm. *: <0.05, **: <0.01. (For interpretation of the references to color in this figure legend, the reader is referred to the web version of the article.)

DNA damage occur, we performed *B* staining (a YSL marker in early embryogenesis (Yang et al., 2011)) in the TUNEL assay slides, and found that the DNA damage was identified in the nuclei of yolk syncytial layer, as well as external tissue layers (Fig. 4E and F). Taken together, these data indicated that *5* knockdown induced DNA damage in the overlying layers of yolk, especially YSL, which eventually resulted in yolk extension defects.

3.5. *53* Rnasel5

Several reports have pointed out that p53 pathway may be associated with the yolk extension defects, and this pathway is also important in the response to DNA damage (Chakraborty et al., 2009; Chen et al., 2006, 2009). Actually, p53 protein was prominently up-regulated in *5* morphants at 24 hpf, compared the control and mRNA-rescue group (Fig. 5A). Two p53 downstream targets, *21* and *B* , were significantly elavated at the RNA level in *5* morphants, indicating knockdown of *5* results in triggered activation of p53 pathway (Fig. 5B).

To determine whether activation of p53 mediates the yolk extension defects in *5* morphants, we injected p53 specific MO into the *5* morphants to inhibit the translation of p53. As shown in Fig. 5C–E, the yolk extension defects in *5* morphants were partially rescued by p53 MO. In addition, the hatching rate and survival rate were also increased in the p53 and *5* MOs co-injected fishes compared to those in *5* morphants (data not shown). To further confirm the role of p53 in the *5*

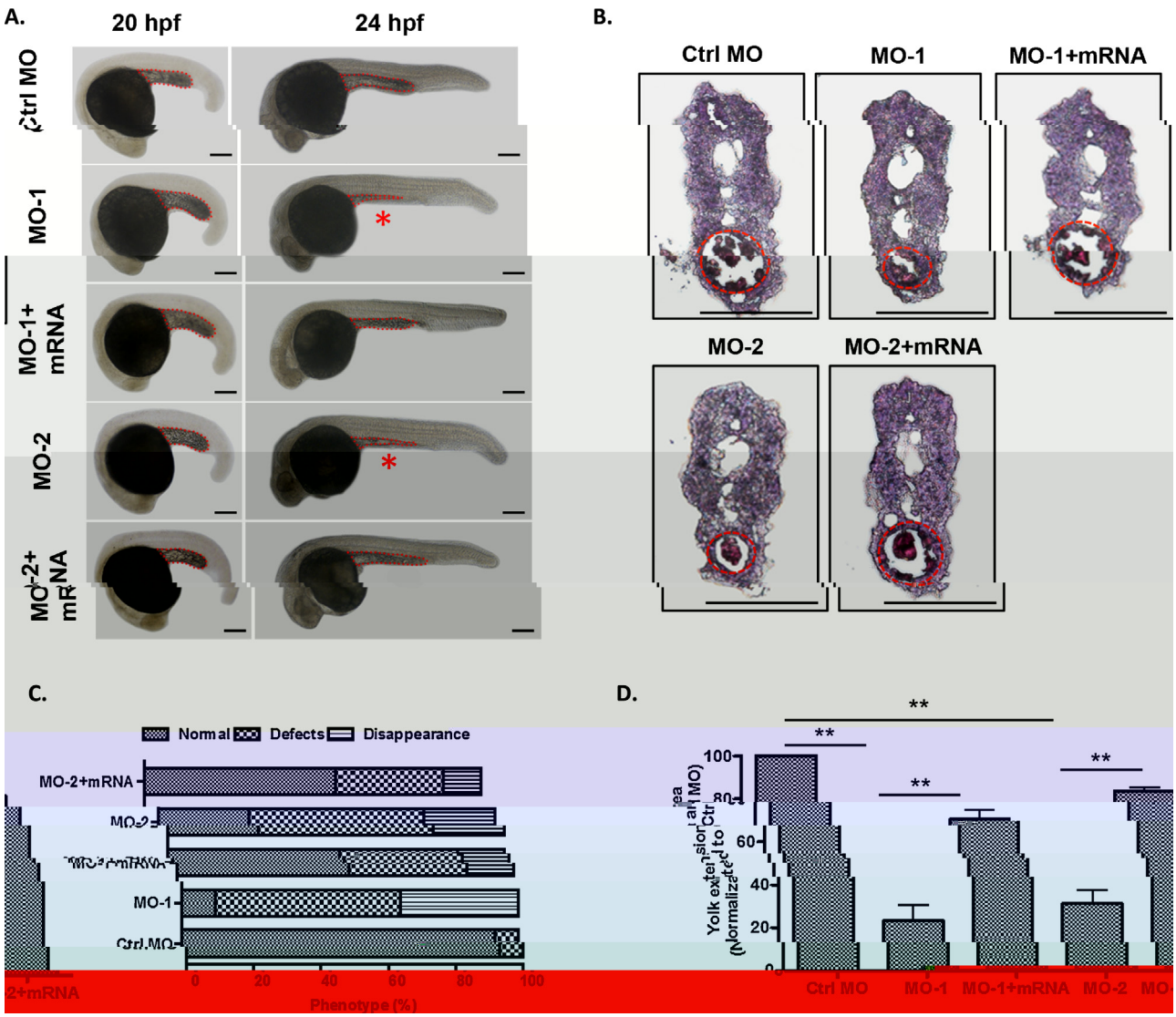

Fig. 3. *5* depletion results in server yolk extension defects. (A) MOs injected embryos were photographed at 20 hpf and 24 hpf. The shrunken yolk extension was identified with asterisk, scale bar = 100 μm. (B) H&E staining was performed on cryosections of the 24 hpf embryos. The yolk extension region was shaped by dotted red line, scale bar 100 μm. (C) Quantitative analysis data of different morphological phenotype (including normal, defects, and disappearance of yolk extension) in morphants. (D) The relative yolk extension region area of different morphants as indicated. All differences are significant, **: <0.01. (For interpretation of the references to color in this figure legend, the reader is referred to the web version of the article.)

depletion-caused yolk extension defects, we introduced a fish line with transgenic *53*^{M214K}, a mutant on p53 DNA-binding domain to block the activation of p53. As expected, knockdown of *5* did not cause the yolk extension defects in these transgenic fishes (Fig. 5F–H). These results indicated that yolk extension defects in *5* morphants is mediated by the p53 pathway.

4. Discussion

To date, five members of the RNASE A family have been identified in zebrafish; however, their functions are less understood. In the present study, we characterized, for the first time, the developmental effects of *5*, a newly identified member of the zebrafish RNASE A family. We found that *5* is a novel regulator of yolk extension development as well as an inducer of DNA damage in the overlying layers of yolk extension. Specifically, knockdown of *5* induced defects in yolk extension and apoptosis via activation of the p53 pathway. In addition, similar to human RNASE5/angiogenin, *5* was also involved in vascular development (Fig. 2F). Certainly, the underlying mechanisms and relationship between different phenotypes need to be further elucidated.

The three structural components of the yolk extension interact with each other in a hierarchical manner to help elongate the cylindrical yolk extension formation (Lyman Gingerich et al., 2006; Virta and Cooper, 2011). Here, we showed that DNA damage caused by *5* deficiency in the overlying layers of yolk extension resulted in shrunken or even disappearance of yolk extension. Several genes have been reported to regulate the yolk extension formation. For example, the *K* (*K*) and *H* *A13* (*H* *A13*) are necessary for the development of yolk extension (Crow et al., 2009; Davidson et al., 2003). It would thus be interesting to investigate the cross-talk and temporal expression of these genes on the development of yolk extension. Moreover, yolk extension defects induced by *5* deficiency occurred at the latter stage of yolk extension formation (20–24 hpf). We therefore propose that *5* may maintain the integrity of yolk extension. Overall, our study reveals that the temporal and spatial expression pattern of *5* is important for the proper development of yolk extension. Of

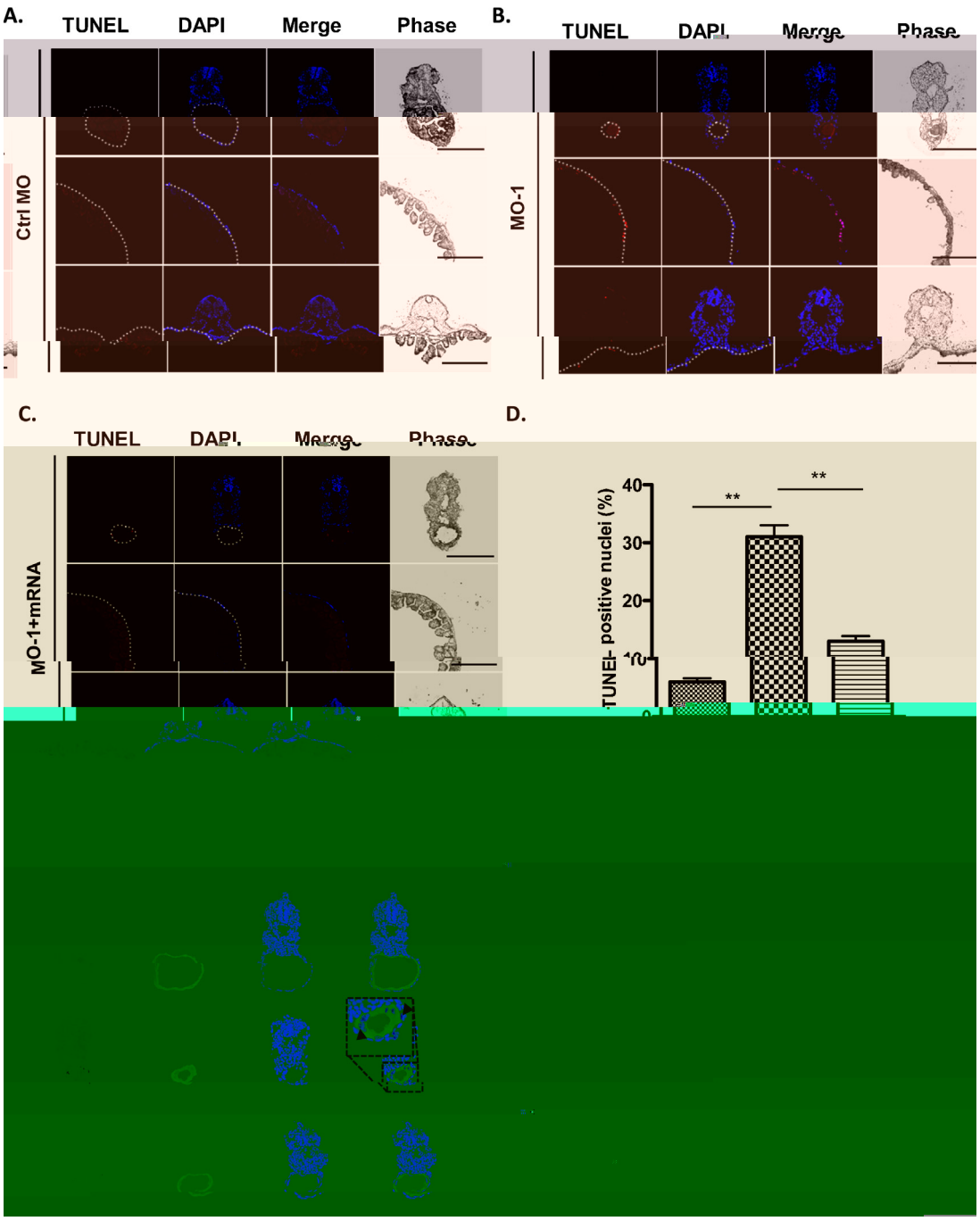

Fig. 4. Yolk extension defects in *5* morphants is resulted from increased DNA damage at the YSL and the external tissue layers. (A–C) TUNEL assay was performed on the cryosections of morphants with TRITC labeled positive cells and DAPI-labeled nuclei, scale bar100 μm. The dot lines indicate the overlying layers of yolk. The upper panel is the cross sections of the middle trunk including yolk extension, the middle and down panels is cross sections of the front trunk including yolk ball. (D) Quantitative analysis data of TUNEL positive nuclei. (E) TUNEL and *B* staining double assay shows DNA damage are most in YSL as well as external tissue layers of yolk. The red arrow show TUNEL positive staining nuclei in external tissue layers, scale bar 100 μm. (F) Quantitative analysis data of TUNEL postive nuclei. All differences are significant, **: <0.01. (For interpretation of the references to color in this figure legend, the reader is referred to the web version of the article.)

course, a tissue specific *5* knock out fish would more than be necessary to further confirm this phenotype.

It is notable that morpholinos are widely used as a tool for gene silencing, but may have off-target effects mediated by p53 activation (Ekker and Larson, 2001), usually resulting in smaller eyes and heads, abnormal notochord and somite, as well as significant neural death at the end of segmentation (1 dpf) (Gerety and Wilkinson, 2011). The key way to distinguish a morpholino's phenotype from off-target effects is to rescue it with mRNA construct of the respective gene in morphants (Robu et al., 2007). Here, we rescued the morphological defects in *5* morphants by co-injection of full-length *5* mRNA. Besides, we used two different MOs targeting distinct sites and detected none apoptotic cells in neural system in *5* morphants at 24 hpf by TUNEL assay (Fig. 4).

Consistently, it has been reported that *A E5*, the human homologue of *5*, can interact with p53 to inhibit its phosphorylation, which in turn increases p53–Mdm2 interaction, and consequently enhances p53 degradation (Sadagopan et al., 2012). *A E5* can also inhibit both mitochondria and death receptor apoptotic pathways to prevent stress-induced apoptosis (Li et al.,

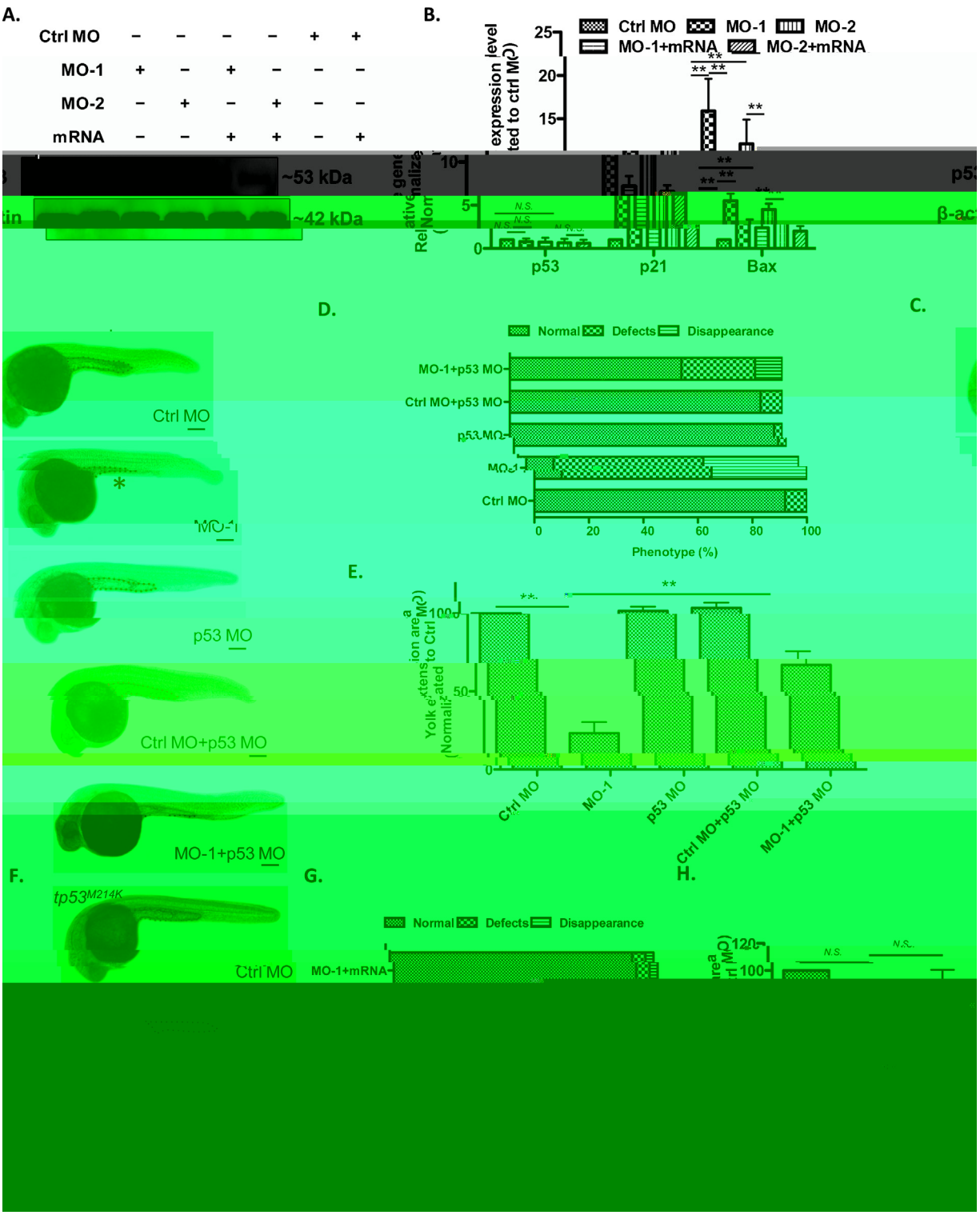

Fig. 5. p53 pathway is activated in *5* morphants and is associated with yolk extension defects. (A) Western blot analysis of p53 protein expression level under different treatments as indicated. (B) RT-qPCR assays of mRNA level of p53 and p53 and its target genes *21* and *B* . (C) Photographs of 24 hpf embryos under different treatments as indicated. The shrunken yolk extension was identified with asterisk, scale bar 100 μm. (D) Quantitative data of different morphological phenotype in each group as indicated. (E) The relative yolk extension area of different groups as indicated. (F) Yolk extension phenotype in *53*^{M214k} transgenic fish line under different treatment, and the quantitative analysis data were analyzed in (G) and (H), scale bar 100 μm.

2010, 2012). In our *5* morphants, p53 protein was significantly up-regulated; however, its mRNA remained unchanged (Fig. 5B), strongly suggesting that *5* may promote the ubiquitination of zebrafish p53 and enhance its degradation through the same pathway instigated by human RNASE5. Our results, on other hand, reflect that zebrafish *5* is a good representative for the study of human RNASE5 in development. Taken together, our data suggest that *5* is essential for the development of yolk extension through repressing the activation of p53.

Acknowledgments

We thank Professor Jinrong Peng (Zhejiang University College of Animal Sciences) for discussions and supports on the study. We thank Core Facilities at Zhejiang University School of Medicine for the technical assistance. We also thank Chi Luo (Dana-Farber Cancer Institute/Harvard Medical School) for critical reading of the manuscript. This work was supported by National Natural Science Foundation of China grants nos. 81372303 and 31170721 (to Zhengping Xu).

References

Chakraborty, A., Uechi, T., Higa, S., Torihara, H., Kenmochi, N., 2009. Loss of ribosomal protein L11 affects zebrafish embryonic development through a p53-dependent apoptotic response. PLoS One 4, e4152.

Chen, G.D., Chou, C.M., Hwang, S.P., Wang, F.F., Chen, Y.C., Hung, C.C., et al., 2006. Requirement of nuclear localization and transcriptional activity of p53 for its targeting to the yolk syncytial layer (YSL) nuclei in zebrafish embryo and its use for apoptosis assay. Biochem. Biophys. Res. Commun. 344, 272–282.

Chen, J., Ng, S.M., Chang, C., Zhang, Z., Bourdon, J.C., Lane, D.P., et al., 2009. p53 isoform delta113p53 is a p53 target gene that antagonizes p53 apoptotic activity via BclxL activation in zebrafish. Genes Dev. 23, 278–290.

Crow, K.D., Amemiya, C.T., Roth, J., Wagner, G.P., 2009. Hypermutability of HoxA13A and functional divergence from its paralog are associated with the origin of a novel developmental feature in zebrafish and related taxa (Cypriniformes). Evolution Int. J. Org. Evolution 63, 1574–1592.

Davidson, A.J., Ernst, P., Wang, Y., Dekens, M.P., Kingsley, P.D., Palis, J., et al., 2003. cdx4 mutants fail to specify blood progenitors and can be rescued by multiple hox genes. Nature 425, 300–306.

Ekker, S.C., Larson, J.D., 2001. Morphant technology in model developmental systems. Genesis 30, 89–93.

Gao, X., Xu, Z., 2008. Mechanisms of action of angiogenin. Acta Biochim. Biophys. Sin. 40, 619–624.

Gerety, S.S., Wilkinson, D.G., 2011. Morpholino artifacts provide pitfalls and reveal a novel role for pro-apoptotic genes in hindbrain boundary development. Dev. Biol. 350, 279–289.

Isken, A., Holzschuh, J., Lampert, J.M., Fischer, L., Oberhauser, V., Palczewski, K., et al., 2007. Sequestration of retinyl esters is essential for retinoid signaling in the zebrafish embryo. J. Biol. Chem. 282, 1144–1151.

Kazakou, K., Holloway, D.E., Prior, S.H., Subramanian, V., Acharya, K.R., Ribonuclease, 2008. A homologues of the zebrafish: polymorphism, crystal structures of two representatives and their evolutionary implications. J. Mol. Biol. 380, 206–222.

Li, Z., Korzh, V., Gong, Z., 2007. Localized rbp4 expression in the yolk syncytial layer plays a role in yolk cell extension and early liver development. BMC Dev. Biol. 7, 117.

Li, S., Yu, W., Kishikawa, H., Hu, G.F., 2010. Angiogenin prevents serum withdrawal-induced apoptosis of P19 embryonal carcinoma cells. FEBS J. 277, 3575–3587.

Li, S., Yu, W., Hu, G.F., 2012. Angiogenin inhibits nuclear translocation of apoptosis inducing factor in a Bcl-2-dependent manner. J. Cell. Physiol. 227, 1639–1644.

Lyman Gingerich, J., Lindeman, R., Putiri, E., Stolzmann, K., Pelegri, F., 2006. Analysis of axis induction mutant embryos reveals morphogenetic events associated with zebrafish yolk extension formation. Dev. Dyn. 235, 2749–2760.

Mizuno, T., Yamaha, E., Kuroiwa, A., Takeda, H., 1999. Removal of vegetal yolk causes dorsal deficencies and impairs dorsal-inducing ability of the yolk cell in zebrafish. Mech. Dev. 81, 51–63.

Monti, D.M., Yu, W., Pizzo, E., Shima, K., Hu, M.G., Di Malta, C., et al., 2009. Characterization of the angiogenic activity of zebrafish ribonucleases. FEBS J. 276, 4077–4090.

Ober, E.A., Schulte-Merker, S., 1999. Signals from the yolk cell induce mesoderm, neuroectoderm, the trunk organizer, and the notochord in zebrafish. Dev. Biol. 215, 167–181.

Pizzo, E., Buonanno, P., Di Maro, A., Ponticelli, S., De Falco, S., Quarto, N., et al., 2006. Ribonucleases and angiogenins from fish. J. Biol. Chem. 281, 27454–27460.

Pizzo, E., Merlino, A., Turano, M., Russo Krauss, I., Coscia, F., Zanfardino, A., et al., 2011. A new RNase sheds light on the RNase/angiogenin subfamily from zebrafish. Biochem. J. 433, 345–355.

Quarto, N., Pizzo, E., D'Alessio, G., 2008. Temporal and spatial expression of RNases from zebrafish (*D*). Gene 427, 32–41.

Robu, M.E., Larson, J.D., Nasevicius, A., Beiraghi, S., Brenner, C., Farber, S.A., et al., 2007. p53 activation by knockdown technologies. PLoS Genet. 3, e78.

Sadagopan, S., Veettil, M.V., Chakraborty, S., Sharma-Walia, N., Paudel, N., Bottero, V., et al., 2012. Angiogenin functionally interacts with p53 and regulates p53-mediated apoptosis and cell survival. Oncogene 31, 4835–4847.

Sheng, J., Luo, C., Jiang, Y., Hinds, P.W., Xu, Z., Hu, G.F., 2014. Transcription of angiogenin and ribonuclease 4 is regulated by RNA polymerase III elements and a CCCTC binding factor (CTCF)-dependent intragenic chromatin loop. J. Biol. Chem. 289, 12520–12534.

Virta, V.C., Cooper, M.S., 2011. Structural components and morphogenetic mechanics of the zebrafish yolk extension, a developmental module. J. Exp. Zoolog. Part B Mol. Dev. Evol. 316, 76–92.

Yang, S.L., Aw, S.S., Chang, C., Korzh, S., Korzh, V., Peng, J., 2011. Depletion of Bhmt elevates sonic hedgehog transcript level and increases beta-cell number in zebrafish. Endocrinology 152, 4706–4717.